

Charge-Phase Qubit in Phase Regime

M. H. S. Am in

D-Wave Systems Inc., 320-1985 W. Broadway, Vancouver, B.C., V6J 4Y3 Canada

A superconducting qubit implementation is proposed that takes the advantage of both charge and phase degrees of freedom. Superpositions of flux states in a superconducting loop with three Josephson junctions form the states of the qubit. The charge degree of freedom is used to readout and couple the qubits. Cancellation of the first order coupling to the environment, at the working point of the qubit, protects it from the decoherence due to charge and flux fluctuations.

Superconducting phase qubits [1, 2, 3, 4, 5] are believed to be superior to charge qubits [6, 7], because of less sensitivity to fluctuations of background charge [8, 9]. Among the former, the three Josephson junction (3JJ) flux qubit [1] has successfully demonstrated coherent Rabi oscillations [2, 3], with a relatively long decoherence time (2.5 s), when probed with a high quality tank circuit [3]. However, there is not yet a clear way to read out a flux qubit in a single-shot measurement, without affecting the coherence of the qubit in the working regime. The dc-SQUID readout is known to be inefficient [10], and is always coupled to the qubit, affecting its coherence [3]. Ref. [10] suggests coupling of an rf-SQUID to the qubit to increase the readout efficiency. Although this seems to solve the problem for a single qubit, scalability of the design is not clear. In other words, since the size of the rf-SQUID should be much larger than the qubit itself (large inductance is necessary for bistability), it is difficult to couple it to only one qubit without affecting the other qubits in a large scale system. This is also a problem for other magnetic field readout and coupling schemes (e.g. coupling to a tank circuit). Moreover, the exponential dependence of the flux tunneling amplitude on the system parameters makes the scalability infeasible. Charge qubits on the other hand, have the advantage of accessibility by electrical currents and less sensitivity to the system parameters, but they suffer from decoherence due to fluctuations of background charges.

A clever design was implemented by Vion et al. [11], demonstrating a very good quality factor (2–10). The reason behind the qubit's success was two-fold. First, it was operated at a so-called "sweet spot", where the fluctuations of both flux and charge affect the qubit only in the second order. Second, the readout circuit was decoupled from the qubit during the operation time. These both were achieved by working in a hybrid charge-phase regime. At the degeneracy point, the state of the qubit is a superposition of charge states. The existing uncertainty in the charge degree of freedom results in some localization of phase, which was employed to distinguish the states of the qubit. Since both charge and phase degrees of freedom were used, the qubit is called a "charge-phase qubit". To reduce the effect of charge noise, Vion et al. chose comparable Josephson and charging energies. An unwanted consequence is a small anharmonicity,

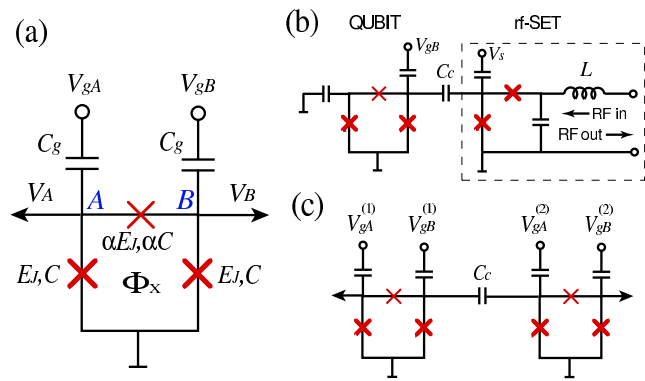


FIG. 1: (a) 3JJ qubit with two gate voltages as a Charge-phase qubit. (b) Single qubit coupled to an rf-SET as a readout device. (c) Two capacitively coupled qubits.

ity, which may cause leakage of quantum information to non-computational states. This is also a problem with qubits made of single Josephson junctions [4, 5].

In this letter, we show that an analogous charge-phase scheme can be implemented for the 3JJ qubit. At the degeneracy point, the two lowest energy quantum states of the qubit are superpositions of left and right circulating current states. Therefore, an uncertainty in the phase-flux space exists, which can lead to localization of the charge degree of freedom, which can be utilized to readout and couple the qubits.

Figure 1a shows the circuit diagram of the system, which is basically a 3JJ qubit; a superconducting loop containing three Josephson junctions, threaded by an external flux close to half a flux quantum ($\Phi_x = 0.5 \text{ f} \text{Wb} = h/4e$). The Josephson energy E_J and junction capacitance C of two of the junctions are the same while the third one's are slightly smaller (E_J and C , with $0.5 < < 1$). In addition, there are voltage sources V_{gA} and V_{gB} capacitively connected to two of the islands (A and B in Fig. 1a), while the third island is grounded. The first two islands are used to couple the qubit to the readout circuit (Fig. 1b) or other qubits (Fig. 1c).

We first study the qubit neglecting the effect of its neighboring circuitry; if the coupling capacitors are much smaller than C , the approximation made is rather good. Having three Josephson junctions removes the necessity

for finite inductance to achieve bistability. Indeed, since the magnetic flux of the qubit is not used for readout (unlike in the 3JJ qubit [1, 2, 3]), the inductance can be extremely small, considerably reducing the decoherence due to magnetic coupling to the environment (e.g. nuclear spins or magnetic impurities). With a small inductance, one can assume the total flux through the loop to be almost equal to the external flux. The phase differences ϕ across the junctions are then constrained by the flux quantization condition: $\phi_1 + \phi_2 + \phi_3 = 2\pi x = 0$. Defining $\phi = (\phi_1 + \phi_2)/2$ and $\phi_3 = (\phi_1 - \phi_2)/2$, the Hamiltonian of the system is (herein $\hbar = 1$)

$$H = \frac{P_x^2 + n_A + n_B)^2}{2M} + \frac{(P_\phi + n_A - n_B)^2}{2M} + U(\phi, \phi_3);$$

where $P_x = i\partial/\partial\phi$ and $P_\phi = i\partial/\partial\phi$ are the momenta conjugate to ϕ and ϕ_3 , $U(\phi, \phi_3) = E_J [2\cos(\phi) + \cos(2\phi_3 + 2\pi)]$ is the potential energy, $M = 2(n_0=2)^2(C + C_g)$, $M_\phi = 2(n_0=2)^2(C + 2C + C_g)$, $n_{A,B} = V_{gA,B}C_g=2e$, and $f = x=0 = 1/2$. At $f = 0$, $U(\phi, \phi_3)$ has degenerate minima at $\phi = 0, \phi_3 = \arccos(1/2)$. The effect of the kinetic term is to make tunneling between the two minima possible. The tunneling matrix element t_1 describes the tunneling within a unit cell. In general, however, there exists a probability of inter-cell tunneling (in an extended phase diagram) with a tunneling matrix element t_2 . The effect of t_2 is to change the energy eigenstates $|j\rangle$ and $|j'\rangle$ to bands with energy eigenvalues

$$E_{0,1}(f; n_A, n_B) = \frac{1}{2} \sqrt{(f)^2 + (n_A, n_B)^2}; \quad (1)$$

where $f = E_J f$, and $|j\rangle$

$$\begin{aligned} (n_A, n_B) = & n_0 \left[1 - \frac{2k_c}{2} \sin^2 n_A + \sin^2 n_B \right. \\ & \left. + \sin^2 (n_A - n_B) \right]^{1/2}; \quad (2) \end{aligned}$$

is a conversion coefficient of 0 (1) [12], $n_0 = (0,0) = 2t_1(1+2)$, $n_1 = t_2 = t_1$, and k_c is a dimensionless coefficient defined in Eq. 4.

At $n_A = n_B = f = 0$, the small flux and charge fluctuations ($f; n_A, n_B$) appear in the second order:

$$\frac{E_{0,1}}{0} = \frac{1}{2} [1 + k_f f^2] \quad (3)$$

$$k_f = \frac{n_A^2 + n_B^2 + (n_A - n_B)^2}{2} ; \quad k_c = \frac{2^2}{(1+2)^2}; \quad (4)$$

Elimination of decoherence due to the first order terms suggests a perfect operation point for the qubit (sweet spot) [11]. The second order charge and flux fluctuations influence the eigenenergies with coefficients k_f/k_c (when

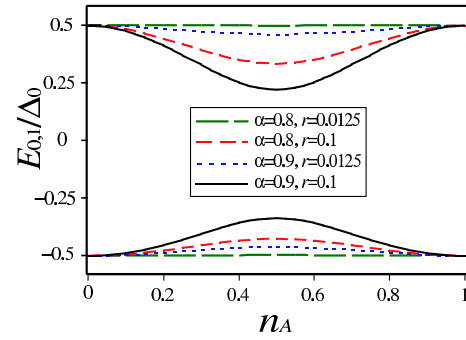


FIG. 2: Energy eigenvalues (E_0 and E_1) as a function of n_A at $n_B = f = 0$, and for different values of α and r . $E_C = E_J$.

1) and $k_f / E_J^2 = 2/9$, respectively. To minimize their effect on coherence, one should make these coefficients small. In the design of 3JJ qubit [1, 9], the parameters are chosen so as to get a vanishingly small (10^{-4}), but large $E_J = 0$ (350). While suppressing the effect of the charge fluctuations quite well, it leaves the qubit sensitive to the fluctuations of flux, even at the sweet spot. In our design, we aim to get a smaller $E_J = 0$, but larger r . Indeed, r is chosen to be small enough to suppress the effect of second order charge fluctuations, but large enough to make the states of the qubit electrically distinguishable, away from the sweet spot.

Figure 2 shows numerical results for E_0 and E_1 (obtained from diagonalization of the Hamiltonian) as a function of n_A , at $n_B = f = 0$, and for different values of α and r . $E_C = E_J$, where $E_C = e^2/2C$ is the charging energy. The agreement with Eqs. (1) and (2) is fairly good, although the exact symmetry between the upper and lower levels does not exist. At $\alpha = 0.8, r = 0.0125$, the eigenvalues show very small dependence on n_A . At $\alpha = 0.9$ and also at larger r , on the other hand, they show strong dependence on n_A . This, as we shall see, is important for our readout and coupling schemes.

The numerical values of α and r are obtained by comparing the curves in Fig. 2 with Eq. (1):

$$\alpha = [E_1(0;0;0) - E_0(0;0;0)]; \quad (5)$$

$$r = \frac{1}{2} \frac{E_1(0;0;0) - E_0(0;0;0)}{E_1(0;0.5;0) - E_0(0;0.5;0)} \quad (6)$$

The dependence of α and r on n_A is displayed in Fig. 3. α decreases with n_A , while r exponentially increases, reaching 1 as $n_A \rightarrow 1$. The latter is understandable because at $n_A = 1$ both barriers are equivalent, leading to equal tunneling matrix elements ($t_1 = t_2$). It is also important to notice that the variations of both α and r with n_A is significantly slower at larger r . This is an important design aspect for large-scale systems (see below). Figure 4 shows how α and r depend on r . Again, their sensitivity to variations of r is smaller at larger r .

The island voltages $V_{A,B}$ are used to couple the qubit to its surroundings. V_A in $|j\rangle$ states is found by tak-

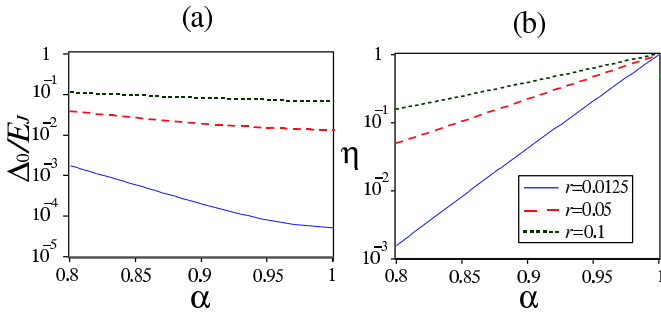


FIG. 3: Dependence of Δ_0 and η on α , for different value of r . The legend is common between the two figures.

ing the derivative of the corresponding eigenenergies with respect to n_A : $V_A = (1-2e)\partial E_{0,1}/\partial n_A$. At $f = 0$, we get

$$V_A = \frac{k_e}{4e} \frac{2}{(n_A; n_B)} [\sin 2 \pi n_A + \sin 2 \pi (n_A - n_B)] \quad (7)$$

The expectation value of the excess charge on the island is then given by $\hbar Q_A = C_V V_A$, where $C_V = C + C_g + [(C + C_g)^{-1} + (C_g)^{-1}]^{-1}$ is the effective capacitance of the island. The voltage and charge of island B can be obtained by replacing A \leftrightarrow B.

When $n_A = n_B = 0; 1 \bmod 1$, the voltages on both islands are zero. The qubit is therefore electrically decoupled from its neighbors. Away from this point, state-dependent voltages appear on the islands, which couple the qubit to its surrounding circuitry. For $\alpha = 1$, the voltage on the island A is maximum when $n_A = \frac{1}{4}$: $V_A = V_{\max} \quad (\alpha=2e)$. An interesting situation is

$$n_A = \frac{1}{4}; \quad n_B = \frac{1}{2} \tan^{-1} \alpha : \quad (8)$$

Then $V_B = 0$, while V_A is close to its maximum. The reverse is also possible replacing A \leftrightarrow B. This makes directional coupling of the qubit to other qubits and to the readout circuit possible (see below).

The charge on the island can be measured by a sensitive electrometer such as a single electron transistor (SET). Figure 1b illustrates a qubit coupled to an rf-SET [13] as a readout device [14]. rf-SET has already been used to read out charge qubits [7], and is known to be faster and more sensitive than a SET. One of the gate voltages of the qubit (V_{gA}) is permanently grounded and the other (V_{gB}) is used to switch the readout on and off. During quantum operations, $V_{gB} = 0$ and therefore there is no coupling to the readout circuit. At the time of readout, a voltage $V_{gB} = e/2C_g$ is applied to make the island voltage state-dependent. This voltage (or the island charge) is detected by the rf-SET device.

Figure 1c shows two qubits coupled via a capacitor C_c , which connects two islands of the qubits. When both gate voltages are set to zero, the charge on the islands of

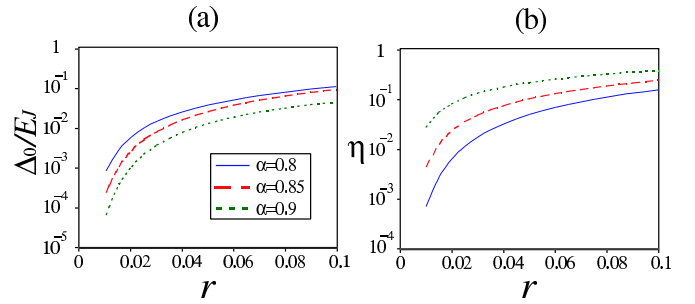


FIG. 4: Δ_0 and η as a function of r .

each qubit will be independent of their states and therefore no coupling exists. When both voltages are set to finite values so that state-dependent charges appear on the qubits' islands, the qubits will be coupled and entanglement will be possible. Truncating the Hilbert space of the system to the two lowest energy states of the qubits and using the spin language, the effective Hamiltonian of the coupled system can be written as

$$H_e = \sum_{i=1,2}^X [i_z^{(i)} + i_x^{(i)}] J_x^{(1)} J_x^{(2)} \quad (9)$$

where $i^{(i)}$ are the Pauli matrices for the i -th qubit and J is the coupling energy. For identical qubits with $\alpha = 1$, and at $f = 0$, to first order in C_c , we find

$$J = C_c \frac{e^2}{2e} \sin 2 \pi n_B^{(1)} \sin 2 \pi n_A^{(2)} : \quad (10)$$

As expected, $J = 0$ when either of n_B and n_A are zero and therefore the two qubits are decoupled. Maximum coupling, on the other hand, is achieved when $n_B^{(1)} = n_A^{(2)} = \frac{1}{4}$. The remaining two islands (A 1 and B 2) can be used to read out the qubits. In order to achieve qubit-qubit coupling without coupling to the readout circuits (and vice versa), the situation described in Eq. (8) (or its reverse) should be used.

It is also possible to couple more than two qubits via a bus island, using similar scheme. Figure 5 illustrates a situation where all qubits are capacitively coupled to an island (which should be small to ensure small capacitance). Each pair of qubits can be then coupled by making their gate voltages nonzero, while other qubits remain decoupled from the island, as long as their gate charge (n_B) is kept at zero [15]. Coupling too many qubits to the island, however, increases the island capacitance, reducing the coupling energy and affecting the quantum operation of all qubits.

In the experiment of Ref. 3, the parameters reported are $E_J = 300$ GHz ($I = 600$ nA), $E_c = 5$ GHz ($C = 3.9$ fF) and $\alpha = 0.8$. The measured value for Δ_0 is 868 MHz. Using these parameters, our numerical calculations give $\eta = 0.0028$ and $\Delta_0 = 0.0028E_J$, in agreement with the experimental findings. A typical set of parameters

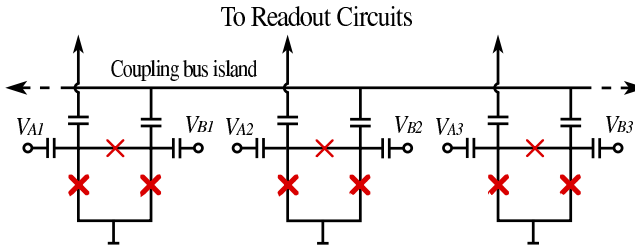


FIG. 5: Controlled coupling of several qubits via a bus island.

that we propose for the present design is $r = 0.85$ and $r = 0.05$, which leads to an 0.1 and $0.026E_J$. Since $r = S^2$, where S is the area of the Josephson junctions, to achieve this regime it is necessary to reduce the area of the larger junctions in Ref. 3 by a factor of

1.77. The resulting E_J will be 170 GHz, leading to 0.44 GHz. Notice an almost one order of magnitude smaller $E_J = 0$, or two orders of magnitude smaller k_f compared to the 3JJ qubit of Ref. 3 (i.e. much smaller sensitivity to the flux fluctuations). As we mentioned before, choosing a large r (compared to the 3JJ qubit) has also the benefit of reducing sensitivity to the system parameters. For example 0 is almost ten times less sensitive to the variations of E_C , E_J , and r , compared to the 3JJ qubit. This indeed becomes crucial for large-scale systems.

For charge fluctuations, we obtain $k_e = 1.4$, more than three times smaller than the equivalent coefficient (5) obtained for the charge-phase qubit of Vion et al. [11]. Thus, the qubit is 3.4 times less sensitive to charge fluctuations. Moreover, the separation between the first two states and the others is much larger than in Vion et al.'s design. With the suggested parameters, we find an anharmonicity coefficient $(E_{21} - E_{10})/E_{10} = 8.3$ ($E_{ij} = E_i - E_j$), more than 40 times the corresponding value (0.2) for Vion et al.'s qubit. This makes the qubit a well-defined two-level system and prevents leakage of quantum information to non-computational states.

Using the above parameters, we find the maximum island voltage V_{max} ($0=2e$) 2.6 V, when $n_A = \frac{1}{4}$. With a capacitance C of a few fF, a charge of $0.1e$ appears on the islands. A charge sensitivity of 4×10^{-5} e/F Hz, with 10 MHz measurement bandwidth, is reported in Ref. 7. The measurement time is limited by the relaxation time τ of the qubit, which is dominantly determined by the fluctuations of the external flux; charge and gate-voltage fluctuations only affect the dephasing time which is irrelevant here. To achieve single shot measurement a $\tau > 0.16$ s is required, which is well below the measured value of 0.9 s in Ref. 2, and other theoretical estimations.

For the coupling energy, the above parameters with $C_c = 1$ fF give $J = 11$ MHz at $n_B^{(1)} = n_A^{(2)} = \frac{1}{4}$. Stronger coupling requires larger C_c and C_c , at the expense of more

sensitivity to charge fluctuations and the necessity for more complicated treatment of the coupling Hamiltonian (beyond the first order perturbation). Magnetic coupling of the qubits is also possible if their self inductance is large enough.

In summary, we have proposed an implementation of a hybrid charge-phase qubit. The qubit loop is similar to the 3JJ qubit. The voltages (charges) of the islands are used to read out and couple the states of the qubits. Each qubit can be read out independently, without affecting the other qubits in a quantum register. With the suggested set of parameters, the effect of the flux

fluctuations is suppressed by almost two orders of magnitude compared to the 3JJ qubit, while the sensitivity to the system parameters is one order of magnitude smaller. The size of the loop can be much smaller than that of the 3JJ qubit, significantly reducing the effect of the coupling to the magnetic environment (nuclear spins, paramagnetic impurities, etc.). Compared to the charge-phase qubit of Vion et al. [11], the proposed qubit has 3.4 times less sensitivity to the charge fluctuations and more than 40 times better anharmonicity. The latter will prevent leakage of quantum information out of the computational states.

The author would like to thank M. Grajcar, J. Hilton, E. Il'ichev, A. M. Aassen van den Brink, A. Yu. Smirnov, and A. M. Zagoskin for stimulating discussions, B. Wilson for critically reading the manuscript, and G. Rose for pointing out the advantage of two control gates.

- [1] J. E. Mooij et al., *Science* **285**, 1036 (1999).
- [2] I. Chiorescu, Y. Nakamura, C. J. P. M. Harmans, and J. E. Mooij, *Science* **299**, 1869 (2003).
- [3] E. Il'ichev et al., *Phys. Rev. Lett.* **91**, 097906 (2003).
- [4] Y. Yu et al., *Science* **296**, 889 (2002).
- [5] J. M. Martinis et al., *Phys. Rev. Lett.* **89**, 117901 (2002).
- [6] Y. Nakamura, Yu. A. Pashkin, J. S. Tsai, *Nature* **398**, 786 (1999); A. Pashkin et al., *Nature* **421**, 823 (2003).
- [7] K. W. Lehnert et al., *Phys. Rev. Lett.* **90**, 027002 (2003).
- [8] Yu. M. Akhlin, G. Schon, and A. Shnirman, *Rev. Mod. Phys.* **73**, 357 (2001).
- [9] T. P. Orlando et al., *Phys. Rev. B* **60**, 15398 (1999).
- [10] L. Tian, S. Lloyd, and T. P. Orlando, *Phys. Rev. B* **67**, 220505 (R) (2003).
- [11] D. Vion et al., *Science* **296**, 886 (2002).
- [12] Ya. S. Greenberg et al., *Phys. Rev. B* **66**, 214525 (2002).
- [13] R. J. Schoelkopf et al., *Science* **280**, 1238 (1998); M. H. Devoret, and R. J. Schoelkopf, *Nature* **406**, 1039 (2000).
- [14] One should make sure that the rf-SET inductor (L in Fig. 1b) does not interfere with qubit's operation.
- [15] In general, applying gate voltage to one qubit, or to the rf-SET (V_s in Fig. 1b), will also affect other qubits. One therefore should apply appropriate voltages to the gates of other qubits to compensate for this.